

## Characterization of Duplex Treated Thresher Chaff Cutter Blades (EN 42 Spring Steel)

Sukhwinder Pal Singh

### ABSTRACT

The nitriding behavior of EN 42 Spring steel was studied on samples previously submitted to heat treatments in order to investigate the effects of the initial microstructure on the thickness and hardness of nitrided layer. Prior to nitriding, samples were fully annealed, quenched and tempered, thus acquiring the lowest and highest hardness respectively. Plasma nitriding was performed at 520 °C for 20 h with a mixture of N<sub>2</sub> and H<sub>2</sub> in a plasma reactor working under floating potential. Structural and mechanical properties of nitrided layers were characterized using SEM/EDAX and X-ray diffraction (XRD), optical microscopy and micro hardness testing. The thicker nitrided layer was obtained for the heat treated samples, in which the nitrided layer is composed of  $\gamma'$ -Fe<sub>4</sub>N and  $\epsilon$ -Fe<sub>2-3</sub>N phases plus a diffusion zone. Plasma nitriding slightly decreased the surface hardness of heat treated samples. Thenitrided depth was also estimated using cross-sectional micro hardness profiles; giving about 3  $\mu$ m for the heat treated and duplex treated substrate.

### 1. INTRODUCTION

Plasma nitriding is a thermo-chemical surface treatment widely used to improve tribo-mechanical properties of engineering components via modification of their surface microstructure [1]. Nitrogen diffusion modifies surface and near surface microstructure producing hard layers with altered mechanical properties [2]. Improvements in tribo-mechanical properties, wear and friction coefficient of steels are attributed to the high surface hardness of nitrided layers [3]. Not only wear resistance is improved, but also corrosion and fatigue resistance may be increased by the same treatment [4-5]. Response to the plasma nitriding not only depends on the process parameters, such as time [6], temperature [7-8], nitrogen potential [9-10] and plasma variables [11], but is also highly dependent upon the substrate alloy type [12], and in the case of given alloy on the initial microstructure [13]. Considering nitrided steel (i.e. substrate plus nitrided layer) as a composite material, load bearing capacity of such composite will depend on the strength or hardness of both the substrate and the nitrided layer. While adequate load carrying capacity requires a high hardness of both substrate and nitrided layer, controlled heat treatment of the substrate prior to nitriding, might allow tuning the changes of the mechanical properties. For example, such treatment could provide high toughness at the inner region and high hardness at component surface. Heat treatment of steel substrates influences their

microstructure which alters nitrogen diffusivity during plasma nitriding. Consequently, the obtained nitrided layers may differ in composition, thickness and mechanical properties. Some investigations have shown that the hardness of nitrided layers increased with plasma nitriding. Most of the studies on the plasma nitriding of EN 42 Spring steel on hardened tempered state and very little work has been done on fully annealed condition. In the present work, the EN 42 steel was plasma nitrided after heat treatment, to evaluate the influence of the initial microstructure on the structure and properties of the nitrided layers.

## 2. Experimental details

### 2.1. Substrate heat treatment and preparation

The samples dimensions are 50mm X 50mm X 5 mm thick were cut from EN 42 Spring steel flat bar. The steel bar in the as-received condition has a hot deformed structure with a hardness of 22 HRC. Its chemical composition given in Table 1 was obtained by optical emission spectroscopy analysis. The samples were heat treated. The schematic diagram of heat treatment is shown in Fig. 1. The heat treatment process where the specimen annealed at 940 °C for 20 minutes. Oil quenched and then double tempering at 250 °C and 540 °C respectively. After the heat treatment and before nitriding, samples were polished carefully with emery papers 80 to 2400 (European FEPA or P-grading). Finally, all samples were ultrasonically cleaned successively in acetone and ethanol then dried under a nitrogen flow before plasma nitriding.

Table 1 Chemical composition of EN 42

EN 42	C	Mn	Si	S	P
Actual (%)	0.8	0.6	0.17	0.014	0.027

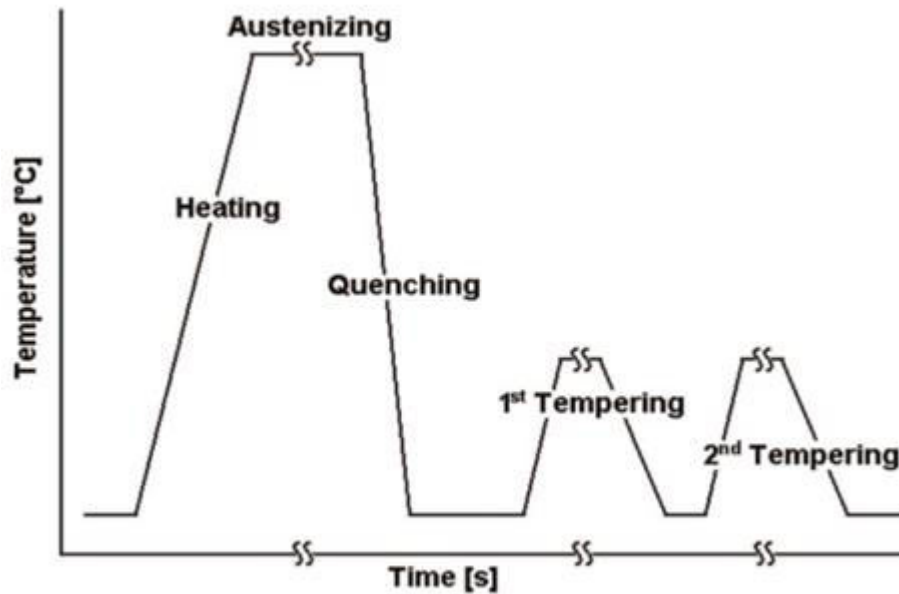


Figure 1 Schematic Diagram for heat treatment process

## 2.2 Plasma nitriding procedure

Plasma nitriding was performed using the NITROPLUS plasma type system, schematically shown in Fig. 2, which is a floating potential RFplasma reactor [14-15]. Plasma was generated using a 25% N<sub>2</sub>–75% H<sub>2</sub> gas mixture in a quartz tube by means of a 13.56 MHz RF power source operating at 750 W working power. The process temperature was 520 °C and the working pressure 8 Pa. Heating was provided by an external electrical furnace which enables the process temperature to be controlled independently from the plasma. In this process, the ion energy is mainly controlled by the furnace wall temperature and the sample surface is not subjected to any sputtering effect. After nitriding for 20 h, the samples were cooled in the vacuum chamber but outside the furnace and the temperature was less than 200 °C after 15 min. In the following, the heat treated sample and after nitriding are denoted A, and T-Nit, respectively.

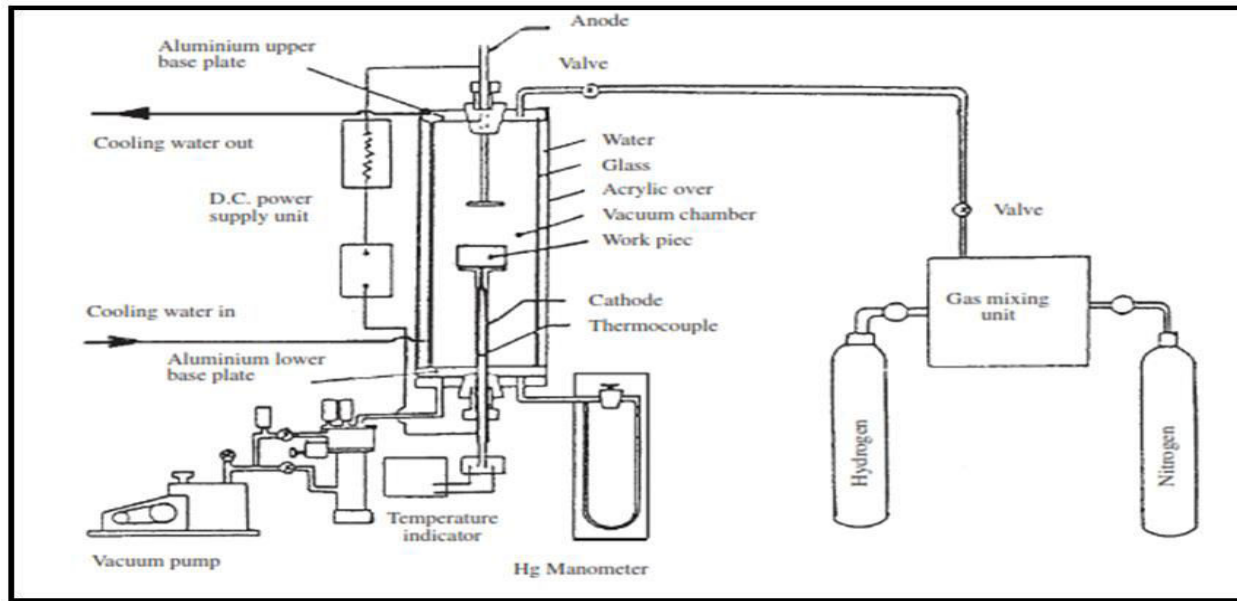


Figure 2 :- Schematic Diagram of Plasma Nitriding

### 2.3. SEM/EDAX Analysis

The microstructure and phase distribution were characterized by SEM and images is composed of coarse martensite structure and carbide formed as results of thermal effects. The surface SEM/EDAX analysis reveals the different proportions of iron, carbon, silicon, phosphorus phases formed on surface at different points.

### 2.4 XRD analysis

Phase composition of the un-nitrided substrates and nitrided layers were studied by X-ray diffraction (XRD) using a XPERT-PRO diffractometer with the Cu-K $\alpha$  radiation ( $\lambda=1.5406 \text{ \AA}$ ) in the Bragg-Brentano configuration operated at 40 KeV and 50 mA. XRD patterns were recorded with step size of  $2^\circ$  and step durations of 4 s at each step in the angular range of  $20^\circ$ – $120^\circ$ . The polished surface was chemically etched with nital reagent for 10s.

### 2.5. Microhardness test

Near surface and cross-sectional hardness was investigated using MDPEL-M400 GL microhardness testing equipped to a Vickers indenter. Measurements were performed under the load 0.1 N (10g) profiles were obtained from the average of three measurements, taken from four distinct regions of cross-section at a given depth. Case depth was determined according to the JIS G0562 standard [16] by measuring distance from the surface to the point that its hardness is about 50 HV higher than the hardness of the substrate. Also the hardness of as received, heat treated and duplex treated measured by Rockwell hardness test.

### 2.5. Optical Microscopy

After plasma nitriding of the substrates, the microstructure along cross-section of sample was observed after polishing. white layer (compound) having thickness 0.3mm. The formation of a compound layer during nitriding significantly enhances the wear properties.

## 3. Results

Fig 3 shows representative microstructure of sample prior to nitriding. The microstructure of sample A consisted of alloy carbides in the ferrite matrix and it has an overall hardness of 55 HRC. Samples T exhibit dispersed carbides in a martensitic structure and their hardness is about 48 HRC. More detailed inspections of the metallographic cross sections in the over-etched condition indicate the excess carbide particles shown in (Fig. 4). Typical optical photographs of cross-sectional microstructure of the T-Nit samples are presented in (Fig. 5). These photographs show formation of diffusion zone on both samples. However in Fig. 5 formation of continuous compound (white) layer on top of the nitrided layer of T-Nit samples is visible. The surface SEM/EDAX analysis reveals the different proportions of iron, carbon, silicon, phosphorus phases formed on surface at different points shown in Fig. (6). The heat treatment process at a certain temperature in order to obtain martensite/austenite structure with further partitioning of carbon from fresh martensite thus stabilizing the latter to martensite transformation. The Surface SEM/EDAX analysis reveals the different properties of C, Si, N, S, Mn, Fe on surface of different points. The nitrided formation in a material shown in Fig (7). A comparison of the XRD patterns before and after nitriding is given in Fig. 6 for the heat treated samples and the duplex treated sample. The diffraction patterns of non-nitrided samples (A and T) show two series of diffraction peaks; one series originating from the steel matrix and the other series

from the dispersed carbide phases. The identified carbide phases are either the SiC or the MnC phases. In fact, several carbide forming elements like C, Si, S and Mn. Besides, they can also form complex carbides such as  $\text{Fe}_2\text{C}_3$ , SiC and MnC. The XRD patterns of samples A and T-Nit shows the peaks of iron nitride and iron carbide. Broadening of the  $\alpha$  peaks for the heat treated sample probably results from the formation of tempered martensite [20]. After plasma nitriding of the heat treated sample, only a few peaks of the original phases are present (T-Nit in Fig. 9). After plasma nitriding an appreciable amount of residual stresses are produced. The main origins of this residual stresses are i) the volumetric expansion due to the nitrogen solution in the iron lattice as solid solution, ii) the formation of nitride precipitates inside the steel matrix and iii) the thermal stresses due to the difference in the thermal expansion coefficients and elastic constants between the nitrided layers and the substrate.

The presense of other iron nitrides peaks indicates that the  $\text{Fe}_4\text{N}$  and  $\text{Fe}_3\text{N}$  phases which are generally reported to be formed on nitrided spring steel shown in (Fig. 9). Cross sectional micro hardness profiles within the nitrided layers are shown in (Fig. 10). The plasma nitrided substrates, the hardness is at maximum on the outward surface and it decreases toward the sample core.. The nitrided layer on the T-Nit substrate exhibits a surface hardness higher than the depth of the substrate. Surface hardness is about 550 HV1 and 390 HV1 in depth for T-Nit sample. In other words, nitriding increases the hardness of T-Nit substrate up to the core hardness. Hardness increasing after nitriding is attributed to the i) solid solution hardening by N atoms ii) formation of fine precipitates of alloy nitrides acting as barriers against movement of dislocations leading to the dispersion-hardening ,iii) presence of compressive residual stresses in the nitrided layer.



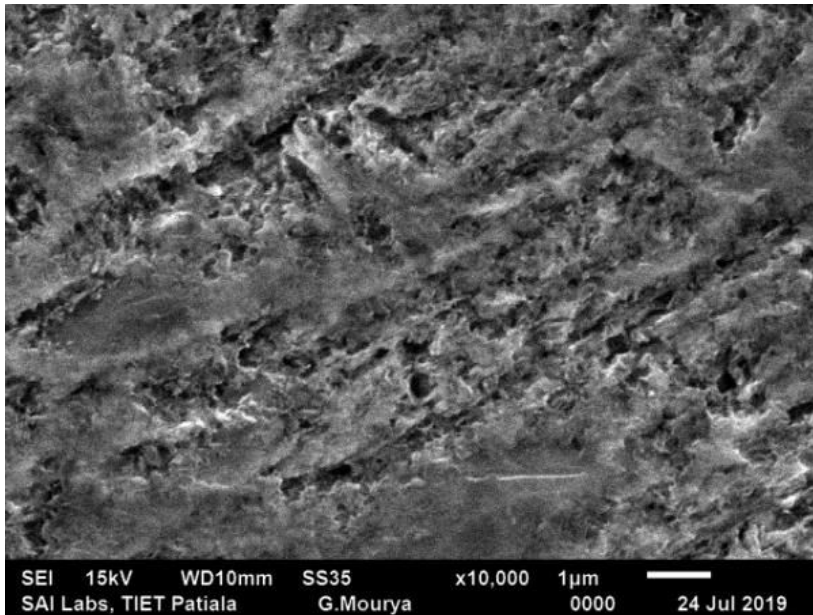


Figure 3. Microstucture prior plasma nitriding.

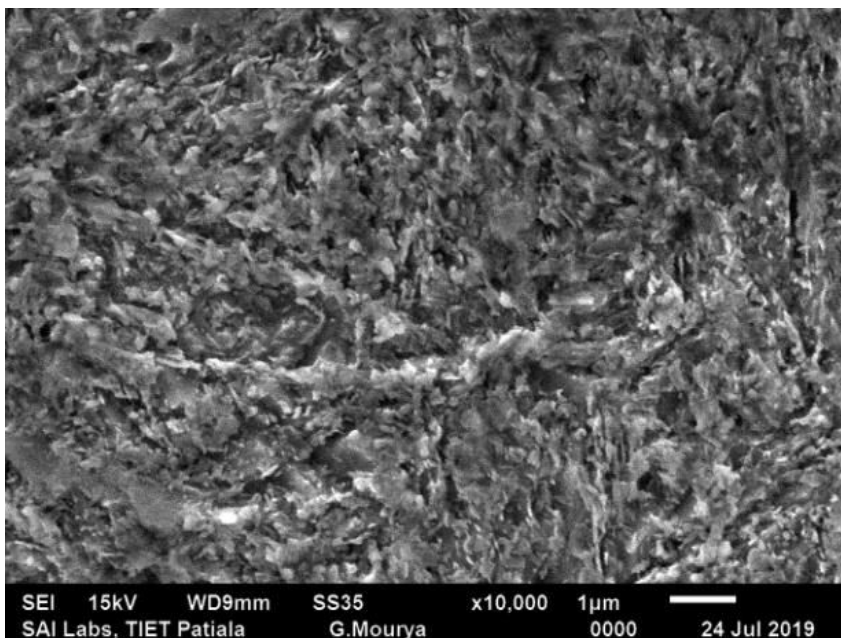


Figure 4 Microstructure after duplex treatment.

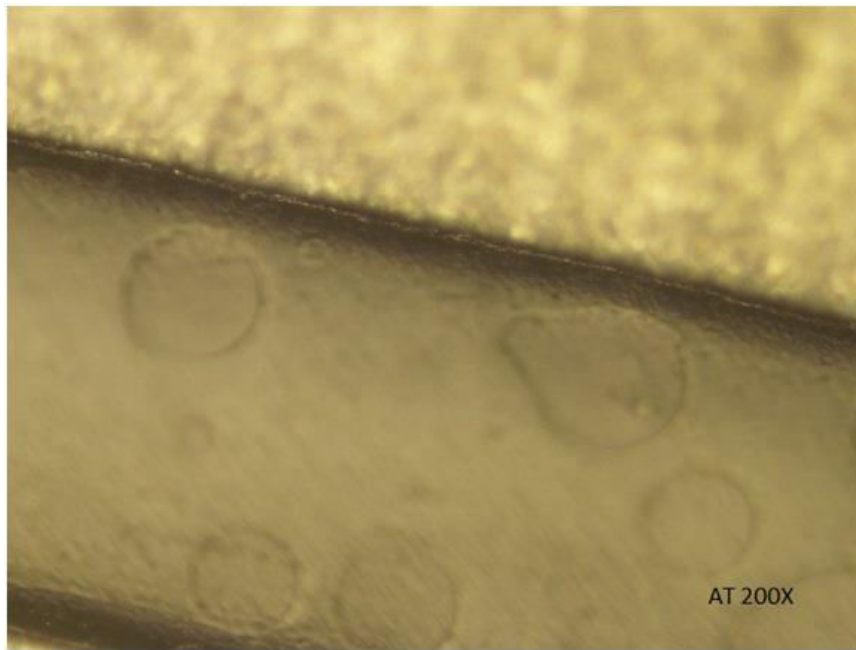


Figure 5 :- Optical Microscopy of duplex treated sample

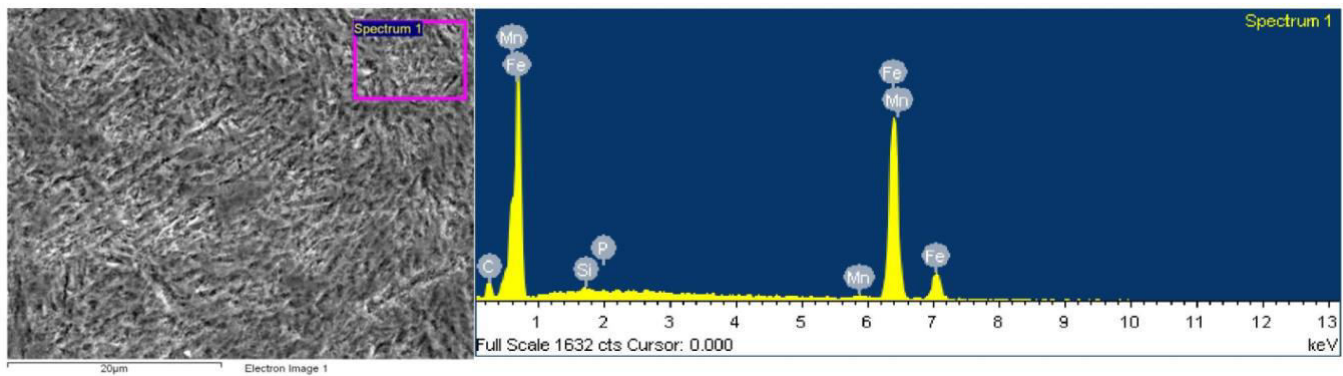


Fig. 6 SEM and EDAX analysis of Heat treated sample of EN 42.



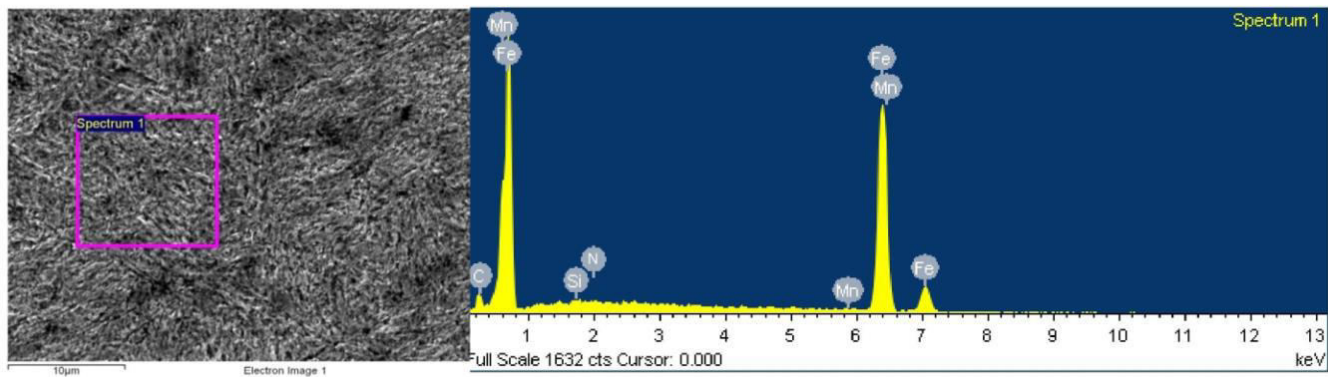


Figure 7 - SEM/EDAX analysis of duplex treated specimen.

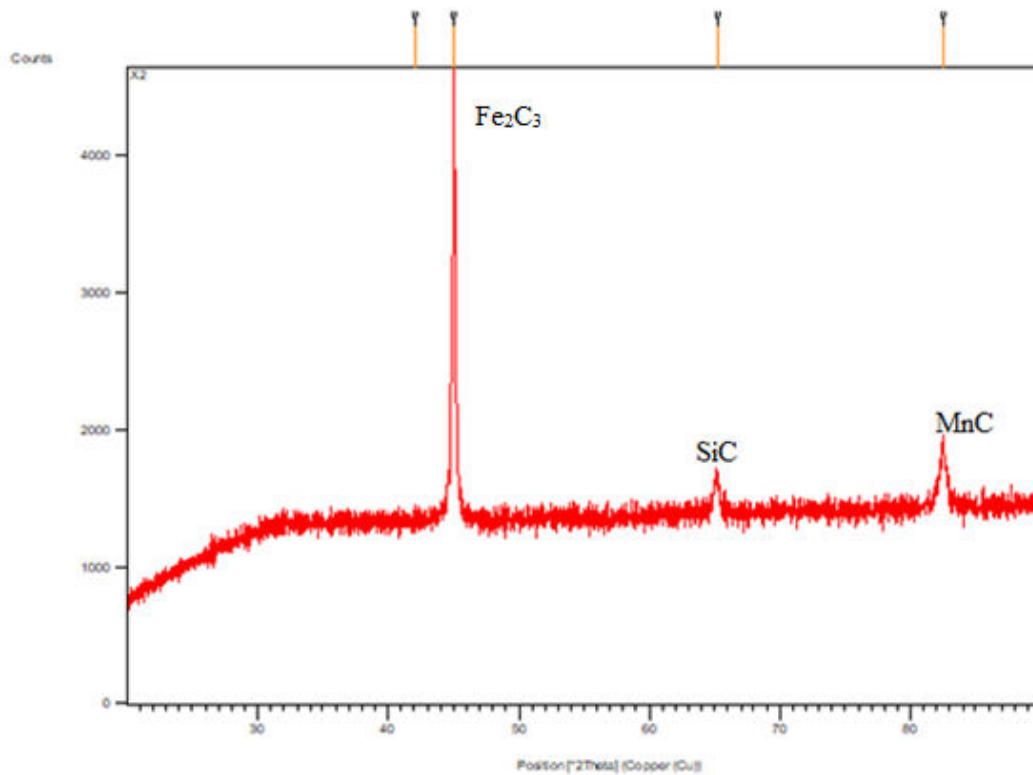


Figure 8 XRD analysis of heat treated sample at 2 theta

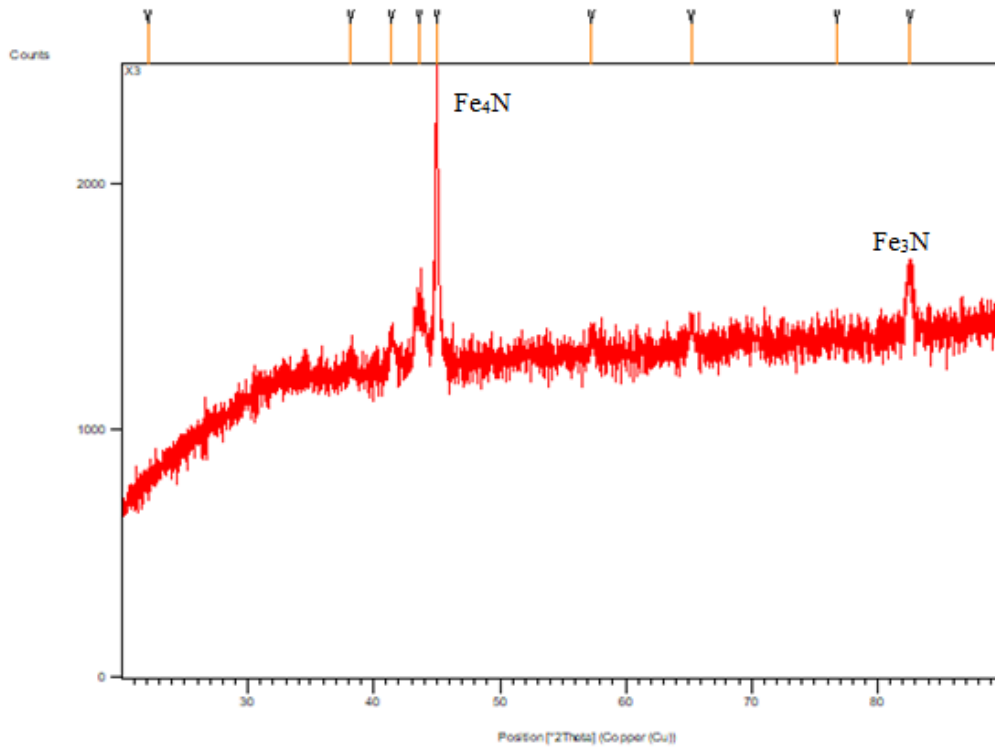


Figure 9 :- XRD analysis of duplex treated samples at 2 theta

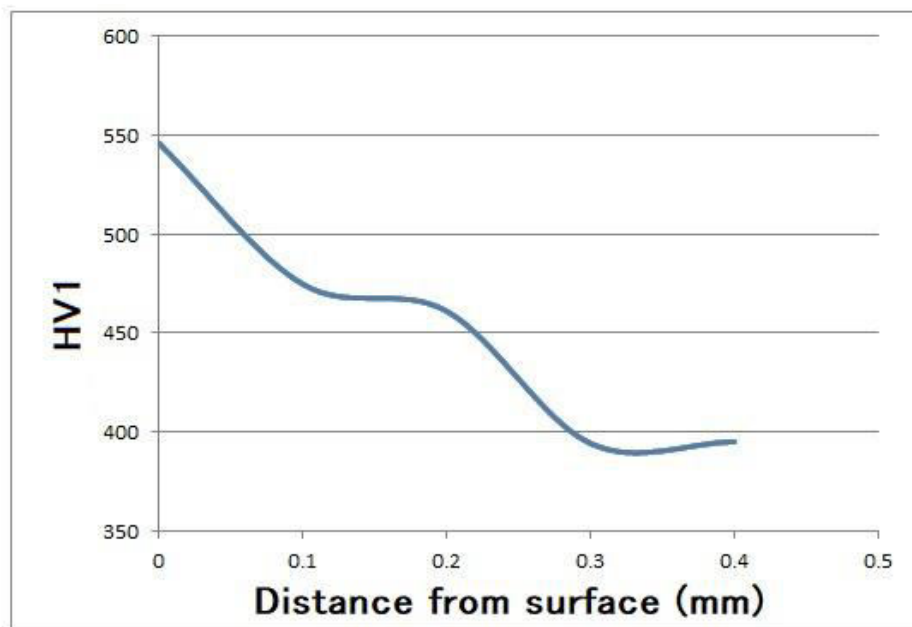


Figure 10 :- Cross-sectional hardness–depth profiles for duplex treated sample

#### 4. Discussion

Evaluation of cross-sectional microhardness depth profiles revealed that the thickness of the nitrided layer for the T-Nit substrate is lesser than surface of substrate. Moreover, the presence of iron nitride, denoted as  $\gamma'$  and  $\epsilon$  phases in the T-Nit samples is an indication of deeper nitrided case depth. The increase of the surface roughness during ion nitriding originates mainly from the differential swelling of the grains. This is due to the fact that the nitrided depth as well as the nitrogen concentration depends on the grain orientation. As the nitrided layer can only expand towards the surface, the deeper nitrided grains exhibit the largest swelling. Usually, another involved mechanism is the sputtering by the nitrogen atoms arriving to the surface during the nitriding process. However, as the nitriding process was performed in a floating potential, the average energy of ions arriving to the surface was only about 15 eV [24]. Therefore, the increased surface roughness may be totally attributed to the volumetric lattice expansion associated to the nitrogen diffusion. Several mechanisms have been proposed for nitrogen mass transfer during plasma nitriding process (see for example references [25]). The overall nitrogen mass transfer is determined by forward reactions involving the interaction of various plasma species, ion-bombardment, gas-absorption, and ion-vacancy-diffusion and backward reactions involving sputtering and denitriding [25]. In plasma nitriding of pure iron in the comparable conditions it is observed that the surface coverage step is faster than nitrogen transport inside the substrate [26]. Therefore, the difference in nitrided depth should be due to the nitrogen transport processes inside the substrate. In order to explain the thicker nitrided layer in the fully annealed samples, one must consider parameters that affect the nitrogen transport processes i.e. nitrogen diffusion coefficient, substrate composition, and the state of residual stresses in the substrate prior to plasma nitriding. The XRD results presented on Fig. 6 and the microstructure shown on Figs. 3 and 4 demonstrate that the main difference between Heat treated (A) and Duplex treated (T-Nit) samples. The atoms of carbon and substitution alloying elements have enough time to diffuse out from the iron matrix before pearlitic transformation. Carbon as an interstitial alloying element has more pronounced effect because it reduces more effectively the number of available interstitial sites for nitrogen (see for example Fig. 7 in reference for the effect of carbon content on the diffusion coefficient of nitrogen in the spring steel). During nitriding of spring steel at high temperature, many precipitates can form in the diffusion zone such like nitrides. Compressive residual stresses introduced by heat treatment to the surface, thus reducing space

between atoms in planes perpendicular to the surface normal. In this way, in-plane compressive residual stresses would retard nitrogen diffusion into the core and therefore lower the nitriding depth.

## 5. Conclusions

The effect of the initial microstructure on the plasma nitriding of EN 42 spring steel steel was investigated. Prior to nitriding, EN 42 spring steel samples were either heat treated or plasma nitrided, leading to two different microstructures; consisting of dispersed alloy carbides in the ferritic and martensitic matrices respectively. The quenched triple tempered samples had higher amount of carbon and alloying elements in the bct- $\alpha$ -lattice, higher level of compressive residual stresses and higher hardness values on surface than the heat treated samples. Samples were nitrided using the 25%N<sub>2</sub>–75% H<sub>2</sub> plasma gas at 520 °C for 20 h using a floating potential RF plasma reactor and thus characterized using XRD and microhardness tester.

1. The case depth of the martensitic matrix being nitrided was 3  $\mu$ m.
2. The smaller nitriding depth observed in the duplex treated (martensitic) was interpreted on the basis of existing compressive residual stresses and remaining of the carbon and alloying elements in the bct- $\alpha$ -lattice, which thus lower the nitrogen diffusion coefficient by trapping nitrogen atoms and forming fine nitrided precipitates.
3. Heat treated specimen SEM results shows the martensite present in material and Duplex treated specimen SEM results show presence Nitrided element.
4. XRD analysis showed that the nitrided layer on top of the duplex treated samples mainly consists of a diffusion zone. Such diffusion zone also appears for the duplex treated sample but preceded by a compound layers made of  $\epsilon$ -Fe<sub>2</sub>–3N and  $\gamma'$ -Fe<sub>4</sub>N.
5. Plasma nitriding of EN 42 spring steel increases the near surface hardness.
6. Plasma nitriding increases the surface roughness. The surface roughness value duplex treated becomes greater than heat treated sample.

## References

- [1] J.M. O'Brien, ASM Handbook, Vol. 4, ASM International, Materials park, 1994.
- [2] M. Keddad, Appl. Surf. Sci. 254 (2008) 2276.
- [3] A. Çelik, Ö. Bayrak, A. Alsaran, İ. Kaymaz, A.F. Yetim, Surf. Coat. Technol. 202 (2008) 2433.
- [4] S.Y. Sirin, K. Sirin, E. Kalucc, Mater. Charact. 59 (2008) 351..
- [5] J.C. Stinville, P. Villechaise, C. Templier, J.P. Riviere, M. Drouet, Surf. Coat. Technol. 204 (2010) 1947.
- [6] C.X. Li, Y. Sun, T. Bell, Mater. Sci. Lett. 19 (2000) 1793.
- [7] L.F. Zagonel, C.A. Figueroa, R. Droppa Jr., F. Alvarez, Surf. Coat. Technol. 201 (2006) 452.
- [8] M.A. Pessin, M.D. Tier, T.R. Strohaecker, A. Bloycec, Y. Sun, T. Bell, Tribol. Lett. 8 (2000) 223.
- [9] M.K. Sharma, B.K. Saikia, A. Phukan, B. Ganguli, Surf. Coat. Technol. 201 (2006) 2407.
- [10] A. Rocha, T. Strohaecker, V. Tomala, T. Hirsch, Surf. Coat. Technol. 115 (1999) 24.
- [11] B. Jeong, M. Ho Kim, Surf. Coat. Technol. 141 (2001) 182.
- [12] C.V. Robino, O.T. Inal, Mater. Sci. Eng. 59 (1983) 79.
- [13] Yu.M. Lakhtin, A.A. Lyubkin, Met. Sci. Heat Treat. 12 (1970) 234.
- [14] J. Perrière, J. Siejka, N. Réмили, A. Laurent, A. Straboni, B. Vuillermoz, J. Apply. Physiol. 59 (1986) 2752.
- [15] L. Marot, A. Straboni, M. Drouet, Surf. Coat. Technol. 142–144 (2001) 384.
- [16] JIS G0562 Standard, Surf. Eng. 11 (1995) 57.
- [17]U. N. Puntambekar, G. S. Grewal, P. B. Joshi and P. Sampath kumaran “Effect of Plasma Nitriding Treatment on Fatigue Life of En-24 steel” (2013)
- [18]A.Poursafar, M. Sabet, S.M.Pesteei, B. Zarifkar, “Influence of Plasma Nitriding on Wear Behavior of AISI D2 Tool Steel”.
- [19]Tatsuhiko Aizawa and Kenji Wasa, “Low Temperature Plasma Nitriding of Inner Surfaces in Stainless Steel Mini-/Micro-Pipes and Nozzles “(2017).
- [20] P.J. Willbur, J.A. Davis, R. Wei, J.J. Vajo, D.L. Williamson, Surf. Coat. Technol. 83 (1996) 250.

- [21] Roselita Fragoudakisa, Stelios Karditsasb, “The Effect of Heat and Surface Treatment on the Fatigue Behavior of 56SiCr7 Spring Steel” (2014)
- [22] Min Shan HTUN, Si Thu KYAW “Effect of Heat Treatment on Microstructures and Mechanical Properties of Spring Steel”(2008)
- [23] M. H. STAIAA, A. FRAGIEL,”Tribological performance of plasma nitride aisi 4140 steel”Vol. 18, N° 3, pp. 97 – 102, 2003.
- [24] L. Marot, Thèse Université de Poitiers, , 2001.
- [25] Y. sun, T. Bell, Mater. Sci. Eng. A. 224 (1997) 33.
- [26] O. Salas, U. Figueroa, J.L. Bernal, J. Oseguera, Surf. Coat. Technol. 163–164 (2003) 339.